

# Microscope Projection Photolithography for Rapid Prototyping of Masters with Micron-Scale Features for Use in Soft Lithography

J. Christopher Love, Daniel B. Wolfe, Heiko O. Jacobs, and George M. Whitesides\*

Department of Chemistry and Chemical Biology, Harvard University, 12 Oxford St., Cambridge, Massachusetts 02138-2902

Received May 2, 2001. In Final Form: June 29, 2001

This paper demonstrates the application of projection photolithography, using a standard commercial microscope, for the generation of masters for soft lithography. The procedure is rapid and convenient and produces features smaller in size (as small as 0.6  $\mu\text{m}$ ) than those available from other methods of rapid prototyping, albeit over a limited area ( $\sim 4 \times 10^4 \mu\text{m}^2$  per exposure). A transparency photomask (prepared using high-resolution printing) is inserted into the light path of the microscope and projected through the microscope objective onto a photoresist-coated substrate. Features on the order of 1  $\mu\text{m}$  can be produced routinely over the area of sharp focus (a circle of radius  $r \approx 100 \mu\text{m}$  with a 100 $\times$  objective) by this method without modification or precise calibration of the microscope. The microscope platform also provides two other useful functions, both characteristic of commercial steppers: step-and-repeat exposures and pattern alignment. The developed photoresist is used as a master for the fabrication of stamps and replica molds for soft lithography. These elements are used in demonstrations of fabrication of microstructures with feature sizes in the range from 1 to 10  $\mu\text{m}$ . Although the technique is limited in the area it can produce in a single exposure, it can fabricate many kinds of structures useful in chemistry, biology, and materials science.

## Introduction

This paper describes the use of projection photolithography using a commercial microscope (microscope projection photolithography, MPP) for the rapid prototyping of masters useful for generating the elastomeric pattern transfer elements (stamps and molds) used in soft lithography. The use of a microscope to achieve size reduction is a familiar (if seldom-used) technique in microlithography.<sup>1–5</sup> The relevance of MPP in the context of soft lithography is that it provides access to micron-scale features without the expense and delay required to produce a chrome mask and without specialized dust-free environments. MPP thus makes it possible for anyone with access to a microscope to generate test patterns and small prototype devices with features a factor of 10 smaller than can be achieved by rapid prototyping techniques based on high-resolution printers.<sup>6–9</sup> We believe that this capability will be particularly useful to scientists (chemists, biologists, materials scientists, physicists) interested

in generating small areas of patterned microstructure for use in research.

Photolithography for production-level processing requires high-quality, expensive equipment and facilities: precision photomasks, mask writers and aligners, steppers, and contamination-free environments. This level of sophistication is necessary for manufacturing multilevel microelectronic devices. For exploratory research, however, it is useful to have methods for generating small numbers of prototype test structures quickly and inexpensively and to be able to optimize these structures through successive iterations. A convenient approach to “rapid prototyping” is to use transparency film photomasks of patterns drawn with CAD software and printed on a desktop printer or high-resolution image setter for contact-mode photolithography in a clean room.<sup>6</sup> Transparency film masks (generated by a printer operating at a resolution of 5080 dots/in. or 5  $\mu\text{m}/\text{dot}$ ) reproduce features as small as 25  $\mu\text{m}$  with only modest distortion.<sup>10</sup>

Other film-based photomasks such as microfiche<sup>7,9</sup> and silver halide film<sup>8</sup> make features between 10 and 40  $\mu\text{m}$  accessible. The need for further miniaturization, and for the capability to fabricate and test individual devices and integrated components with features  $\leq 1 \mu\text{m}$ , requires new tools; a wide array of fields (microfluidics, microanalysis, MEMS, cell biology) would benefit from simple procedures for rapidly prototyping structures with feature sizes in the range between 0.5 and 10  $\mu\text{m}$ .

Microscopes are used routinely for resolving and magnifying features with dimensions  $\geq 0.2 \mu\text{m}$ ; the

\* Corresponding author: Tel (617) 495 9430; Fax (617) 495 9857; E-mail gwhitesides@gmwhitesides.harvard.edu.

(1) Berg, H. A. M. v. d.; Ruigrok, J. J. M. *Appl. Phys.* **1978**, *16*, 279–287.

(2) Behm, J. M.; Lykke, K. R.; Pellin, M. J.; Hemminger, J. C. *Langmuir* **1996**, *12*, 2121–2124.

(3) Brady, M. J.; Davidson, A. *Rev. Sci. Instrum.* **1983**, *54*, 1292–1295.

(4) Feuer, M. D.; Prober, D. E. *IEEE Trans. Electron. Devices* **1981**, *ED-28*, 1375–1378.

(5) Palmer, D. W.; Decker, S. K. *Rev. Sci. Instrum.* **1973**, *44*, 1621–1624.

(6) Qin, D.; Xia, Y.; Whitesides, G. M. *Adv. Mater.* **1996**, *8*, 917–919.

(7) Deng, T.; Tien, J.; Xu, B.; Whitesides, G. M. *Langmuir* **1999**, *15*, 6575–6581.

(8) Deng, T.; Arias, F.; Ismagilov, R. F.; Kenis, P. J. A.; Whitesides, G. M. *Anal. Chem.* **1999**, *72*, 645–651.

(9) Deng, T.; Wu, H.; Brittain, S. T.; Whitesides, G. M. *Anal. Chem.* **2000**, *72*, 3176–3180.

(10) Features as small as 10  $\mu\text{m}$  can be produced by the imagesetter although reproducible patterns are limited to straight lines and dots with periodicity larger than the feature size (see Figure 2a). There is substantial variation in the uniformity of shape and size of individual features, however. Arbitrary designs show significant distortions of the original shapes.

resolving power of a microscope objective is set by the theoretical limits of diffraction,  $R = \lambda/(2NA)$  (where NA is the numerical aperture of the objective), and by practical limits including the optical alignment of the microscope, the quality of the lenses, and the predominant wavelengths of light used to image a specimen.<sup>11</sup> The optical system of a microscope can be used in reverse to project a reduced image onto a sample with the same resolution. The reducing power of the optics within a standard microscope, when used in reverse (i.e., for size reduction) and when combined with high-resolution transparency photomasks, provides a rapid, inexpensive, and widely accessible technique for generating features as small as  $0.6 \mu\text{m}$  over a patterned area of  $\sim 10^4 \mu\text{m}^2$ . The roughness of the edges of linear features in photoresist after development is  $< 0.2 \mu\text{m}$ . In many applications, the convenience of this method for prototyping small features compensates for the limited area of the image generated.

MPP was developed and optimized with acetate film or tape masks in the 1970s and 1980s. Palmer and Decker used MPP to pattern features in photoresist as small as 500 nm; these features were transferred into an underlying metal film by metal anodization.<sup>5</sup> Freuer and Prober demonstrated MPP in combination with liftoff to produce 200 nm wide metal lines and superconducting microbridges.<sup>4</sup> More recently, Boxer and co-workers have used MPP to pattern photosensitive materials trapped in lipid bilayer partitions on a surface to generate pixelated, gray-scale images.<sup>12</sup> Experiments have shown that the limit of resolution,  $R$ , of the technique approaches the theoretical limit of  $R = \lambda/(2NA)$  (where NA is the numerical aperture of the objective) when (i) the exposing light is in the near-UV ( $< 450 \text{ nm}$ , where the photoresists are most sensitive) and (ii) the focus is corrected for longitudinal chromatic aberrations between the focus in the visible spectrum (450–750 nm) and the near-UV spectrum (300–450 nm).<sup>1,3</sup>

We concentrate here on the utility and convenience of MPP for generating masters of the types required for soft lithography.<sup>13,14</sup> Patterns in photoresist fabricated using MPP make it straightforward to cast poly(dimethylsiloxane) (PDMS) stamps and replica molds for soft lithography,<sup>13–15</sup> microfluidic systems,<sup>16,17</sup> patterns and systems for cell biology,<sup>18–21</sup> solid-state and organic microelectronic devices,<sup>22</sup> and other micron-scale systems. Using transparency film masks in a commercially available reflected-light microscope, we can routinely generate patterns with

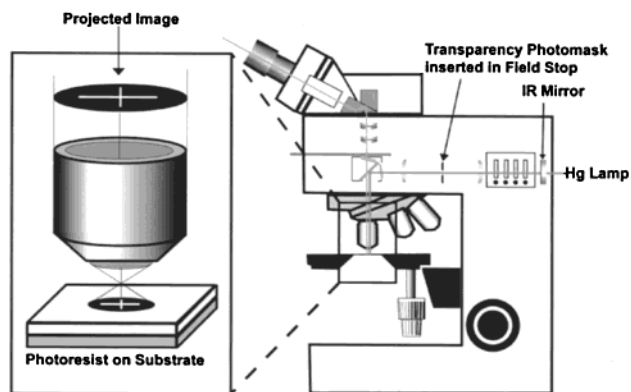


**Figure 1.** Schematic diagram for the adaptation of the microscope for projection photolithography. The photomask is placed in the field stop (or diaphragm) of the microscope; the mask is in an optical plane conjugate to the substrate on the microscope stage. The light, passing through the mask and the objective, exposes the photoresist on a substrate on the stage. The pattern transferred from the mask to the photoresist is reduced by the objective. Since the image of the mask is in an optical plane conjugate to the surface of the substrate, the mask image is focused when the substrate is in focus.

feature sizes in the range of sizes down to  $1 \mu\text{m}$  with good resolution and down to  $0.6 \mu\text{m}$  with increased edge roughness, distortions, and occasional defects. The area in which an image can be generated in a single exposure with a  $100\times$  objective is limited to a circle with a radius of  $\sim 100 \mu\text{m}$  by uneven light intensities at the edges of the image and optical distortions of the features in the mask near the edges.

### Configuration of the Microscope

Figure 1 illustrates schematically the configuration of the microscope and the point of insertion for the mask for projection photolithography. We designed the masks using a CAD tool (Freehand 8.0, Macromedia, San Francisco, CA) and printed both positive and negative images of the masks using a high-resolution image setter with 5080 dpi resolution (Linotype-Hell Herkules Imagesetter, Page-works, Cambridge, MA). Each mask was cut into a circle (11 mm in diameter) with features patterned over a circular area  $\sim 5 \text{ mm}$  in diameter in the center of the mask. We inserted the mask behind the field diaphragm (10 mm maximum diameter). In the optical system of the microscope, the field diaphragm is a conjugate optical plane to the plane of the substrate on the stage. We used a mercury arc lamp (80–100 W) as the source for exposures. The mercury lamp includes emission lines at 435, 405, and 365 nm; broad-band photoresists are sensitive in this spectral region.<sup>23</sup> We achieved the highest resolution using a water immersion lens ( $100\times$ ,  $NA = 1.2$ ) with a glass coverslip over the photoresist layer to protect the resist from water. Distilled water was used as the immersion media.

We controlled the exposure time by switching two neutral density filters (one in the diaphragm module and one in the filter magazine) in and out of the optical path. We filtered the light source with an IR mirror to cut off all wavelengths above 700 nm. Typical exposure times through a  $100\times$  water immersion objective varied from 5 to 12 s with the lamp output set at 80 W and the aperture diaphragm closed to 0. Variations in the lamp intensity, aperture setting, and mask design required a dose array

(11) For a detailed description of microscopy illumination techniques and the resolving power of microscopes, see *Molecular Expressions Microscopy Primer* (<http://micro.magnet.fsu.edu/primer/anatomy/illumination.html>).

(12) Kung, L. A.; Groves, J. T.; Ulman, N.; Boxer, S. G. *Adv. Mater.* **2000**, *12*, 731–734.

(13) Xia, Y.; Whitesides, G. M. *Annu. Rev. Mater. Sci.* **1998**, *28*, 153–184.

(14) Xia, Y.; Whitesides, G. M. *Angew. Chem., Int. Ed. Engl.* **1998**, *37*, 550–575.

(15) Xia, Y.; Rogers, J. A.; Paul, K. E.; Whitesides, G. M. *Chem. Rev.* **1999**, *99*, 1823–1848.

(16) McDonald, J. C.; Duffy, D. C.; Anderson, J. R.; Chiu, D. T.; Wu, H.; Whitesides, G. M. *Electrophoresis* **2000**, *21*, 27–40.

(17) Jeon, N. L.; Dertinger, S. K. W.; Chiu, D. T.; Choi, I. S.; Stroock, A. D.; Whitesides, G. M. *Langmuir* **2000**, *16*, 8311–8316.

(18) Chen, C. S.; Mrksich, M.; Huang, S.; Whitesides, G. M.; Ingber, D. E. *Science* **1997**, *276*, 1425–1428.

(19) Chiu, D. T.; Jeon, N. L.; Huang, S.; Kane, R.; Wargo, C. J.; Choi, I. S.; Ingber, D. E.; Whitesides, G. M. *Proc. Natl. Acad. Sci. U.S.A.* **2000**, *97*, 2408–2413.

(20) Ostuni, E.; Kane, R.; Chen, C. S.; Ingber, D. E.; Whitesides, G. M. *Langmuir* **2000**, *16*, 7811–7819.

(21) Takayama, S.; McDonald, J. C.; Ostuni, E.; Liang, M. N.; Kenis, P. J. A.; Ismagilov, R. F.; Whitesides, G. M. *Proc. Natl. Acad. Sci. U.S.A.* **1999**, *96*, 5545–5548.

(22) Rogers, J. A.; Bao, Z.; Meier, M.; Dodabalapur, A.; Schueller, O. J. A.; Whitesides, G. M. *Synth. Met.* **2000**, *115*, 5–11.

(23) The optics in the microscope are glass which are compatible with the near-UV wavelengths emitted by the Hg lamp.

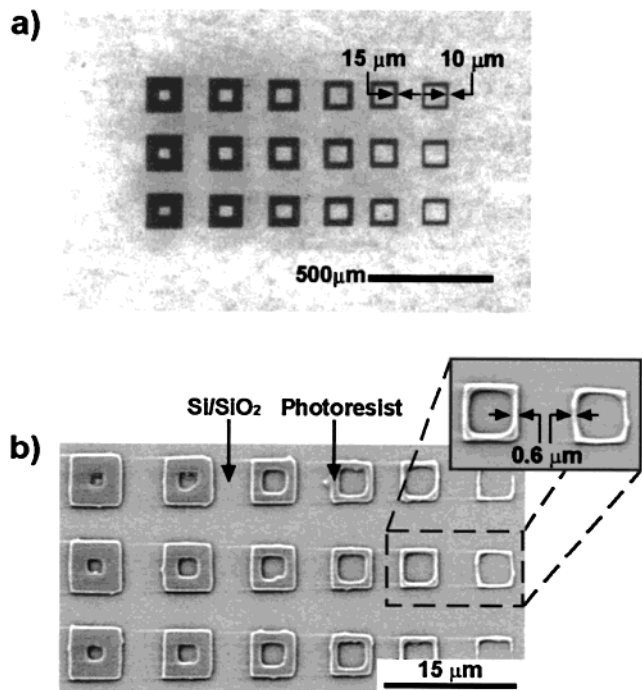


**Figure 2.** Minimum critical dimension of the technique. (a) Optical micrograph of the transparency photomask. (b) Scanning electron micrograph (SEM) of the corresponding developed photoresist pattern on Si/SiO<sub>2</sub> after reduction through a 100 $\times$  water immersion objective. The smallest line widths are 0.6  $\mu$ m. Both 10 and 15  $\mu$ m line widths in the original photomask were reduced to 0.6  $\mu$ m; thus, the reduction in size of the 10  $\mu$ m lines is limited by diffraction.

to calibrate the exposure time for each new mask and substrate. The development time was fixed at 45 s to determine the optimal exposure time. A typical time required to create an array of 100 separate exposures (using manual control of the microscope stage to step the image over the surface) over an area of 1–2 cm<sup>2</sup>, including an initial dose array,<sup>24</sup> was 1 h. All of the experiments were conducted on a closed-door laboratory benchtop (that is, not in a clean room but in a room restricted to instruments) under a red light or a dim ambient fluorescent lamp.

## Results and Discussion

**Analysis of the Technique.** A commercial stepper is capable of repeating an exposure across a surface with high resolution and accurate registration. We have evaluated the ability of the microscope to meet these requirements.

**Resolution of the Minimum Critical Dimension.** The pattern on the transparency photomasks is reproduced accurately on the photoresist with a reduction of size determined by the objective and by the internal optics of the microscope. Figure 2 shows an example of a transparency film photomask inserted into the illumination path of the microscope and the corresponding pattern transferred into a layer of positive photoresist (1.3  $\mu$ m thick) supported on a silicon wafer. The line widths of the boxes in the transparency mask range from 50 to 10  $\mu$ m (Figure

2a).<sup>10</sup> The line widths of the mask features larger than 15  $\mu$ m are reduced by a linear factor of 25 when transferred to the photoresist layer on the substrate. The smallest linear features observed in the photoresist (using a high-resolution transparency mask) are approximately 0.6  $\mu$ m; patterns with these feature sizes begin to show significant distortions.

The linear factor of reduction is 4 times less than the nominal power (100 $\times$ ) of the objective. In an unmodified Leica DMRX microscope, an additional lens between the photomask and the objective (Figure 1) is a normal part of the optics designed for uniform sample illumination.<sup>11</sup> The lens expands the image of the mask inserted in the field diaphragm by 4 times (linear) prior to reduction through the objective. Unfortunately, the field diaphragm is the most accessible image plane conjugate with the substrate on the stage without significant alterations to the microscope. Another microscope with a different optical design and appropriate light filters should be able to generate smaller lines.

The reduction of the smallest line width from 10 to 0.6  $\mu$ m suggests that resolution is limited by diffraction. The resolution limit due to diffraction is  $R = K\lambda/NA$ . The parameter,  $K$ , is approximately 1 for a single-layer resist on a reflective substrate,<sup>25</sup> so the expected limit of resolution is  $\sim 0.6 \mu$ m using the microscope configuration described above.

In the unmodified commercial microscope, the inability to achieve the nominal, linear scaling factor of the objective sets a practical limit for the level of light filtering necessary to obtain minimum feature sizes. With a maximum linear scaling factor of 25 $\times$  attained using a 100 $\times$  objective, features below 0.6  $\mu$ m after reduction would require feature sizes on the original mask that are below 15  $\mu$ m. Since arbitrary designs on transparency masks cannot be printed with critical dimensions below 25  $\mu$ m without distortions of the pattern, the light source does not need additional filtering to lower the maximum wavelength during exposure below  $\sim 700$  nm.

**Area of a Single Exposure.** The maximum field of exposure is limited in area by the optical system of the microscope and the objective. Based on geometrical optics, the diameter of the projected image is related to the diameter of the original mask by a scaling factor that depends on the distance of the mask from the objective and the other optical lenses in the path. The maximum diameter of the original mask at the field stop diaphragm is 10 mm. Based on the linear reduction factor measured empirically from the images patterned in the photoresist, the maximum diameter of the area patterned was equal to  $D_M/R_{\text{eff}}$ , where  $D_M$  is the diameter of the projected mask and  $R_{\text{eff}}$  is the effective power of reduction given the position of the mask and the optical system. In our experimental setup,  $R_{\text{eff}}$  was 4 times less than the stated power of the objectives as described above. The parameter  $R_{\text{eff}}$  will vary on other microscope configurations depending on the optics used and the distance of the mask from the objective. In our configuration with the 100 $\times$  immersion lens, the maximum diameter of the reduced image was 400  $\mu$ m.

We found, however, that the typical diameter of the area patterned with reasonable fidelity is approximately 2 times smaller than the maximum diameter possible because the light source is nonuniform. The intensity profile of the light source is Gaussian with the maximum concentric with the optical axis. The intensity drops off

(24) The dose array is a series of exposures on a photoresist-coated substrate where the time of exposure is varied to determine the optimal exposure time for the given microscope configuration, mask, and sample. An array is prepared for each new session of lithography and each new mask used. The development time is a fixed length of 45–60 s for all exposures.

(25) Moreau, W. M. *Semiconductor Lithography: Principles, Practices, and Materials*; Plenum Publishing Corp.: New York, 1988.

near the edges of the field, and features at the edges of a large mask often do not reproduce well. We limit our features to the center region ( $\sim 5$  mm diameter) of the mask to reduce distortions in the image transferred into the photoresist. The maximum diameter of the area patterned with this design constraint is  $200\ \mu\text{m}$ . The use of objectives with lower magnification powers produces larger areas of exposure with a corresponding decrease in minimum feature sizes when using the transparency masks.

**Mask Defects.** A key limitation of the transparency film used for the photomasks is the presence of small air bubbles trapped randomly inside of the polymer sheet. The size of the bubbles vary from  $<1$  to  $30\ \mu\text{m}$ . The bubbles scatter the light projected through the mask and interfere with the transfer of the pattern onto the photoresist. The locations of defects in photoresist patterns after development correspond with the positions of the bubbles in the transparency photomask. The locations and sizes of the bubbles vary with each mask. The defects are most apparent in patterns where the dimensions of the features on the mask or the spacing of the features are approximately equal in size to the bubbles.

**Registration for Multilayer Fabrication.** The microscope inherently provides the features necessary for the registration of multiple patterned layers that are found in conventional mask aligners, i.e., optically monitored position feedback and  $x$ - $y$ - $\theta$  translation control. Figures 3a and 3b demonstrate the ability to overlay patterns for multiple-step fabrications using the manual microscope translation stage. The test pattern was generated by exposing independently two patterns: the alignment markers and the cross connecting the markers. The accuracy in alignment by hand is  $0.35\ \mu\text{m}$  on average in both  $x$  and  $y$  directions. The angular alignment is achieved by rotating the stage for coarse corrections and adjusting the field diaphragm to rotate the inserted photomask itself for fine corrections. This two-step angular alignment process is accurate to  $<0.5^\circ$ .

**Step-and-Repeat Patterning.** Although the area of each individual exposure is limited, multiple copies of the image are created by translating, i.e., stepping, the sample and repeating the exposure multiple times. Because of the limited depth of focus of the objectives, variations in the thickness of the resist, and the unevenness of the substrate and the microscope stage, the focus of the projected image required adjustments after each step. Figure 3c shows an array of images from a single patterned transparency, in developed photoresist, generated by this step-and-repeat method. Exchanging the mask between exposures allows one to generate several variations of a prototype on a single substrate; this capability is also found in a conventional stepper used in microfabrication.

**Fabrication of Microstructures Generated by MPP and Soft Lithography.** We have evaluated the practicality and convenience of MPP for soft lithography by generating several representative structures.

**Replica Molding.** MPP produces simple masters from which replicas for soft lithography can be molded; we have exposed a honeycomb pattern onto photoresist as a demonstration. Figure 4a–c shows the reproduction of the pattern from transparency film to photoresist (Shipley 1813) master to a PDMS replica. The  $50\ \mu\text{m}$  line widths on the mask were reduced to  $2\ \mu\text{m}$  in the photoresist pattern using a  $100\times$  objective. A PDMS prepolymer was cast onto the photoresist master to generate a soft replica with an inverted relief of the features.

**Microcontact Printing.** A PDMS replica molded from the photoresist master also is useful as an elastomeric

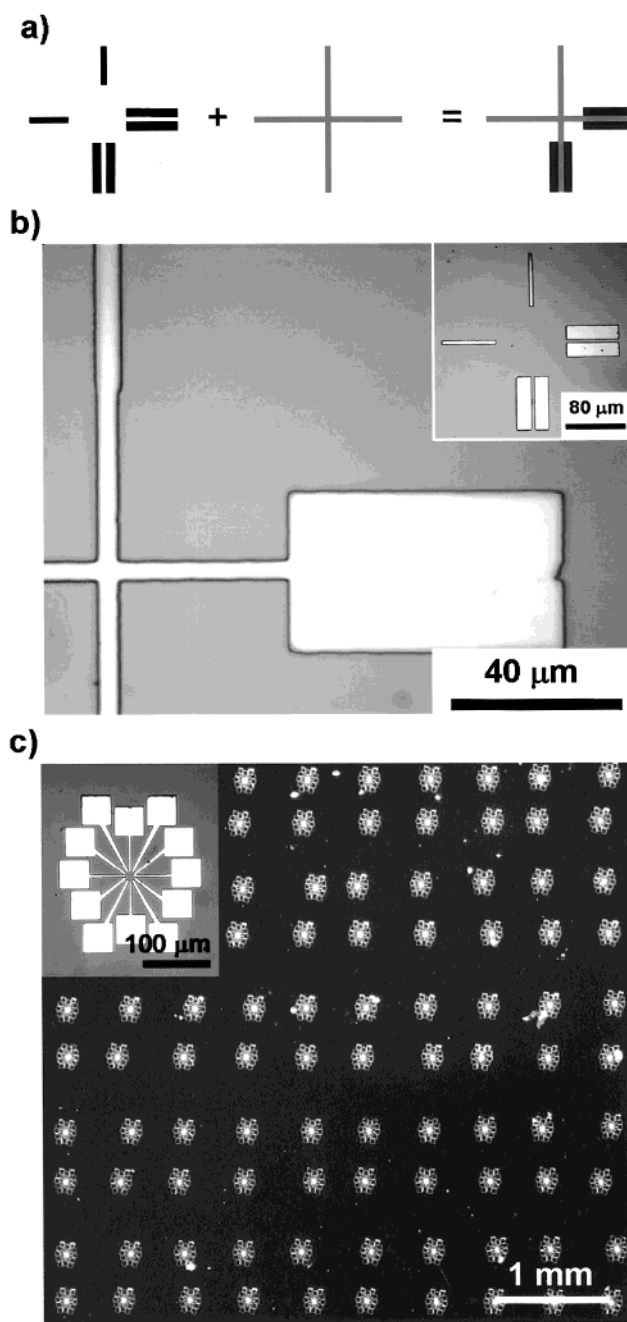


**Figure 3.** Using the microscope as a mask aligner/stepper. (a) Schematic diagram showing the two patterns exposed independently to generate a two-exposure, registered pattern. The alignment marks were exposed first, followed by the cross connecting the marks. With this series of exposures, the registration in  $x$ ,  $y$ , and  $\theta$  were measured. (b) Optical micrograph of the edge of one set of overlaid exposures. The average accuracy of alignment in  $x$ ,  $y$ , and  $\theta$  was  $0.35\ \mu\text{m}$  and better than  $0.5^\circ$ , respectively. The inset shows the first exposure of alignment marks patterned in photoresist prior to alignment for the second exposure of the connecting cross. (c) Optical micrograph (dark field illumination) of an array of images in photoresist generated by step-and-repeat exposures. The test pattern was a set of electrodes with  $50 \times 50\ \mu\text{m}$  contact pads and with leads tapering down to  $\sim 3\ \mu\text{m}$ . The repeated images were exposed through a  $40\times$  objective onto Shipley 1813 photoresist. (The indirect lighting highlights the edges of the topographically patterned photoresist. This method of illumination also highlights some dust and other contaminants present on the surface after development.) The inset shows a close-up of one of the exposures in the photoresist imaged with bright field (direct) illumination.

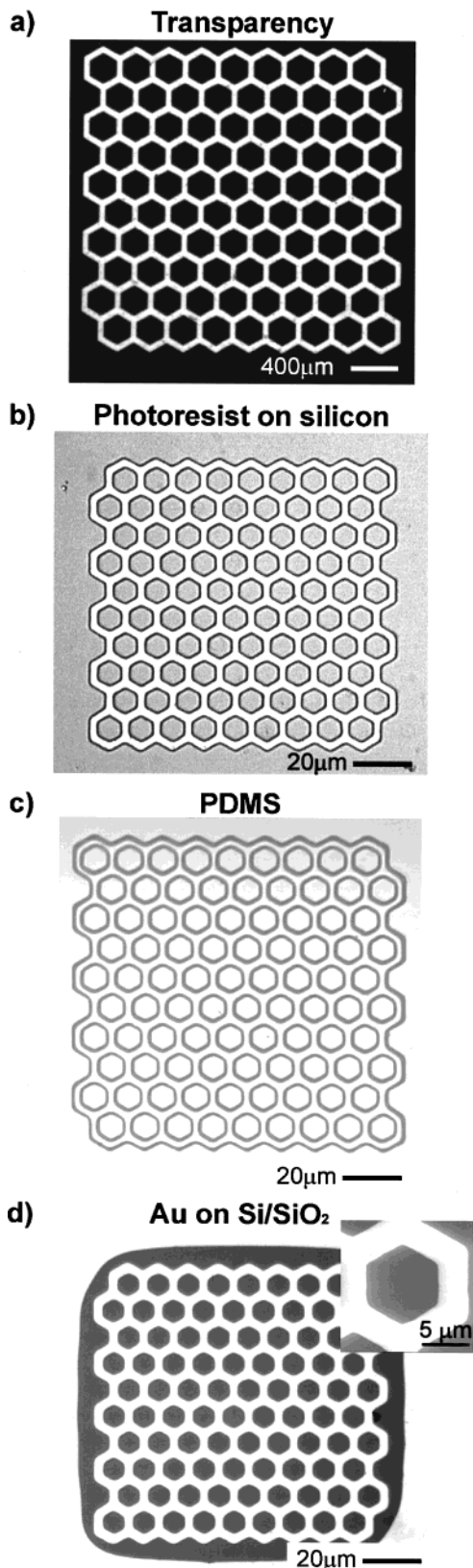


**Figure 4.** Replica molding and  $\mu$ CP using a master generated by MPP. (a) Optical micrograph of the transparency photomask. (b) Optical micrograph of the resulting pattern in photoresist after exposure using projection photolithography through a  $100\times$  objective. The linear dimensions of the pattern are reduced by  $25\times$ . (c) Optical micrograph of a PDMS replica molded against the photoresist master. (d) Optical micrograph of the honeycomb structure formed on gold by microcontact printing hexadecanethiol followed by etching. The inset is a scanning electron micrograph (SEM) of one of the hexagons at the edge of the array.

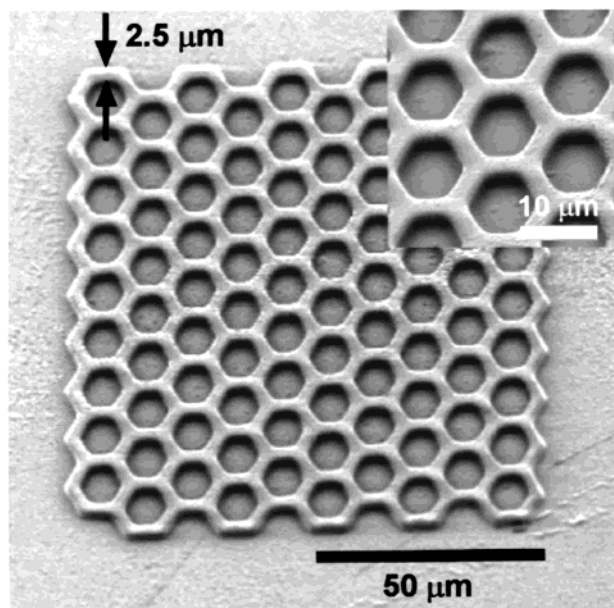


**Figure 5.** SEM of a polyurethane (PU) structure. The PU replica was molded by  $\mu$ TM on a glass slide from a PDMS mold. The mold was cast from a SU-8 master produced by MPP using a  $100\times$  objective. The PU prepolymer was cured for 30 min under a UV lamp.

stamp for microcontact printing ( $\mu$ CP), a principal technique in soft lithography.<sup>13,14</sup> We printed a hexadecanethiolate SAM on gold using the PDMS replica of the hexagonal array. A mild ferri/ferrocyanide etch transferred the pattern printed on the gold surface into the gold film (Figure 4d).<sup>26</sup> We observed slight diffusional spreading of the SAM during the printing process that led to minimum features slightly larger than those on the master or on the PDMS replica.

*Microtransfer Molding.* A key technique in soft lithography is microtransfer molding ( $\mu$ TM).<sup>27</sup> In this technique, a liquid prepolymer fills in the recessed features in a PDMS mold, and the mold is placed into contact with a substrate. After UV curing, the mold is removed, leaving a negative replica of the mold in polymer on the substrate. Figure 5 shows a polyurethane replica of a honeycomb structure. The minimum line width is  $2.5\ \mu\text{m}$ ; this value matches the minimum line width of the PDMS mold. The photoresist master was fabricated using SU-8, a negative photoresist.

*Arrays of Polymeric Microlenses.* Figure 6 shows an array of microlenses fabricated by microcontact printing on a thin gold film and selective wetting of the patterned surface. We generated a photoresist master composed of two offset square arrays of crosses and circles. A PDMS replica was cast to use as the stamp for microcontact printing. 1-Mercaptohexadecanoic acid was stamped to pattern hydrophilic areas on the surface with the pattern desired for the microlenses. The substrate was then dipped in a solution containing hexadecanethiol, a compound that forms a hydrophobic alkanethiolate SAM, to ensure good contrast in the wettability of the surface. Dip coating the substrate in SU-8-2 photoresist generated the lenses. The SU-8 polymer selectively wets the hydrophilic regions on the surface. Figure 6 shows an array composed of two offset square lattices of lenses generated on a thin film of

(26) Xia, Y.; Zhao, X.-M.; Kim, E.; Whitesides, G. M. *Chem. Mater.* **1995**, *7*, 2332–2337.

(27) Zhao, X.-M.; Xia, Y.; Whitesides, G. M. *Adv. Mater.* **1996**, *8*, 837–840.

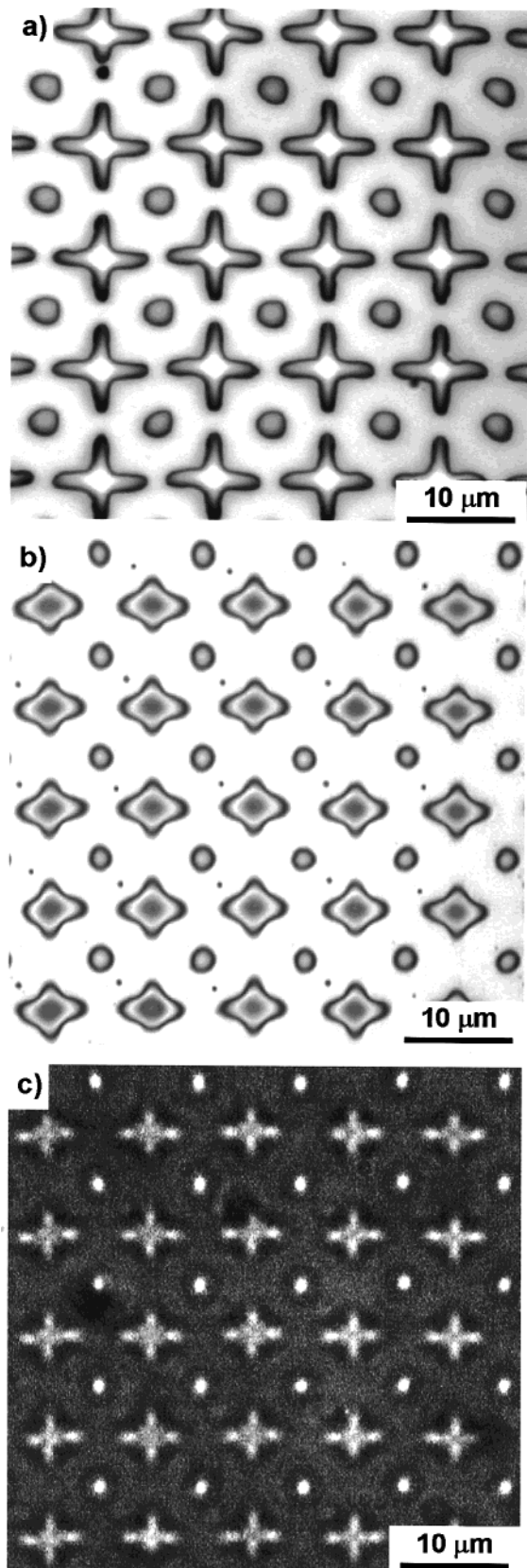


**Figure 6.** Fabrication of an array of microlenses. (a) Optical micrograph of a section of the photoresist master generated by MPP and used as a mold for creating the PDMS stamp for  $\mu$ CP. (b) Optical micrograph of polymeric microlenses fabricated by selectively wetting a SU-8 photoresist on a thin film of SAM-patterned gold on a glass slide. (c) Transmission optical micrograph imaged through the polymeric microlenses. A point light source was transmitted through the array of lenses and the image captured in the focal plane of the lenses.

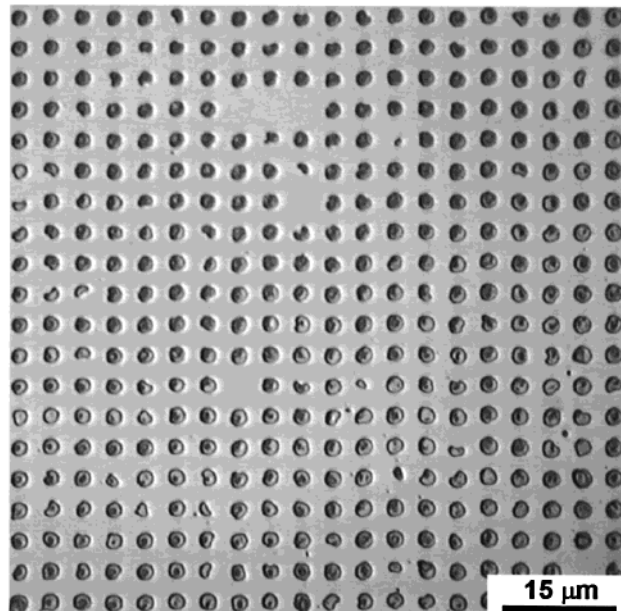


**Figure 7.** Optical micrograph of an array of iron oxide nanoparticles deposited on the surface by selective wetting.

gold on a glass slide.<sup>28</sup> Figure 6b shows the image of a point light source transmitted and focused through the array of lenses shown in Figure 6a. Arrays of microlenses have applications as diffractive optical elements and as image-reducing lenses for unconventional photolithography.<sup>29</sup>

*Arrays of Magnetic Particles.* Figure 7 shows an array of iron oxide nanoparticles deposited onto a gold substrate in  $2\ \mu\text{m}$  dots spaced by  $2\ \mu\text{m}$ . The surface was patterned as described earlier by microcontact printing with a hydrophilic SAM followed by selective wetting of the surface with a ferrofluid.<sup>30</sup> Note that the defects and partially formed spots in the array result from bubbles trapped in the original photomask and are transferred from the photoresist master to the SAM-patterned surface. (See section entitled Mask Defects.)

*Electrical Microcontact Printing (e- $\mu$ CP).* The masters generated by MPP also are suitable for patterning trapped charges in thin-film electrets.<sup>31</sup> A PDMS stamp ( $7\ \text{cm} \times 7\ \text{cm}$  wide and  $3\ \text{mm}$  thick) patterned in bas-relief from the MPP master was coated with a thin film of gold ( $80\ \text{nm}$ ) on an adhesion layer of chromium ( $7\ \text{nm}$ ). We then placed the stamp in contact by hand with a thin film of PMMA ( $70\ \text{nm}$ ) on a p-type silicon wafer. To pattern charge in the PMMA film electret, we applied a voltage pulse between the PMMA-coated silicon substrate and the metal-coated stamp. We have not yet completely characterized the process that results in patterned charge, but it appears that injected charge is trapped in the polymer layer and localized to the areas of contact of the stamp with the polymer film. The trapped charges modify the surface potential of the film; the surface potential was imaged using Kelvin probe force microscopy.<sup>32,33</sup> Figure

(28) Previously, techniques for rapid prototyping could not produce both arbitrary lattice types and shapes of lenses with critical dimensions on the micron scale.<sup>6–9,29</sup>

(29) Wu, M. H.; Whitesides, G. M. *Appl. Phys. Lett.* **2001**, *78*, 1775–1777.

(30) Palacin, S.; Hidber, P. C.; Bourgoin, J.-P.; Miramond, C.; Fermon, C.; Whitesides, G. M. *Chem. Mater.* **1996**, *8*, 1316–1325.

(31) Jacobs, H. O.; Whitesides, G. M. *Science* **2001**, *291*, 1763–1766.

(32) Jacobs, H. O.; Knapp, H. F.; Muller, S.; Stemmer, A. *Ultra-microscopy* **1997**, *69*, 39–49.

(33) Jacobs, H. O.; Knapp, H. F.; Stemmer, A. *Rev. Sci. Instrum.* **1999**, *70*, 1756–1760.

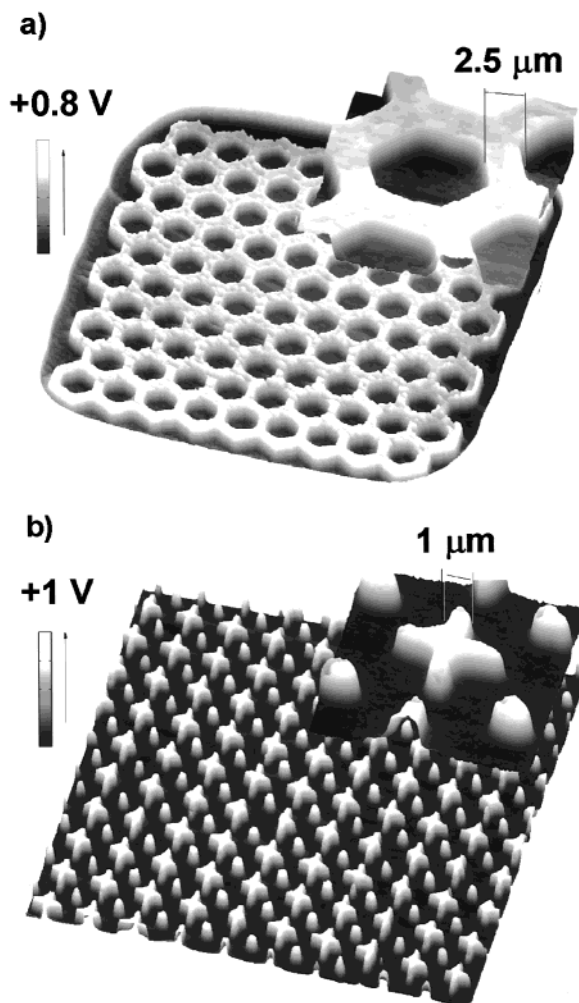


**Figure 8.** Kelvin probe force microscopy images of the surface potential of a pattern of charge in PMMA generated by  $e\text{-}\mu\text{CP}$ . To pattern the charge in both images, we applied a potential of 15 V for 5 s between the conducting stamp and the PMMA-coated silicon chip. The surface potential was imaged 1–2 h after charging the polymer film. (a) Surface potential image of a positively charged hexagonal lattice pattern. The pattern was generated using a gold-coated PDMS stamp carrying a grid of  $2.5\ \mu\text{m}$  wide lines that were  $1.3\ \mu\text{m}$  high (Figure 4c). (b) Surface potential image of positively charged  $5\ \mu\text{m}$  wide crosses and  $1\ \mu\text{m}$  wide dots. The pattern was generated using a gold-coated PDMS stamp carrying crosses and dots that were  $1.3\ \mu\text{m}$  high. The stamp was molded from the photoresist master shown in Figure 6a.

8 shows representative images of the surface potential above the PMMA film after patterning.

### Conclusion

Microscope projection photolithography is a convenient technique for creating masters from which to mold replicas in PDMS (or other elastomers) for soft lithography. Feature sizes on the order of  $1\text{--}10\ \mu\text{m}$  are easily accessible using  $40\times$  and  $100\times$  objectives and transparency photomasks. The limit of resolution is  $0.6\ \mu\text{m}$  with no modifications to the microscope and with transparency masks printed at 5080 dpi. Currently, there are no other rapid prototyping techniques for soft lithography that yield submicron resolution with arbitrary designs. PDMS replicas of the photoresist masters are useful for microcontact printing, microtransfer molding, and the other soft lithographic techniques that require an elastomeric stamp or mold. The advantages of this technique are that (i) it uses widely

available equipment with no significant modifications, (ii) it uses inexpensive, readily available photomasks, (iii) it does not require specialized facilities, and (iv) it routinely provides resolution of  $1\text{--}2\ \mu\text{m}$ . The key disadvantage of the technique is that it produces the patterns over limited areas ( $\sim 4 \times 10^4\ \mu\text{m}^2$  with the highest reduction factor) in single exposures, although step-and-repeat procedures obviate this problem for repetitive patterns.

### Experimental Section

**Materials.** Au ( $>99.99\%$ ), Cr ( $>99.99\%$ ),  $\text{Na}_2\text{S}_2\text{O}_3$ ,  $\text{K}_3\text{Fe}(\text{CN})_6$ ,  $\text{K}_4\text{Fe}(\text{CN})_6$ ,  $\text{CH}_3(\text{CH}_2)_{15}\text{SH}$ , acetone, methanol, propylene glycol methyl ether acetate (PGMEA), and hexamethyldisilazane (HMDS) were used as received. Microposit 1805 and 1813 photoresist (Shipley Co. Inc., Marlborough, MA), Microposit 351 developer (Shipley Co. Inc., Marlborough, MA), and SU-8 photoresists (Microchem Co., Newton, MA) were used as received. Fresh gold substrates for microcontact printing were prepared by thermal or electron beam evaporation on silicon wafers ( $(100)$ , p- or n-type, Silicon Sense, Nashua, NH) or glass slides. Typically, the thin films were coated with  $1\text{--}2\ \text{nm}$  of Cr as an adhesion layer and  $15\text{--}35\ \text{nm}$  of gold.

**Fabrication of the Transparency Masks.** The masks were designed using a CAD software tool (Freehand 8.0, Macromedia, San Francisco, CA). Each mask was drawn within a circle  $11\ \text{mm}$  in diameter, and the patterns were centered in a circle  $\sim 5\ \text{mm}$  in diameter within the mask to minimize uneven exposures due to nonuniform light intensity at the edges of the illumination field. The mask was printed on transparency film (Agfa Alliance film, Agfa-Gevaert, Mortsel, Belgium) using a high-resolution image setter (Linotype-Hell Herkules 5080 dpi, Pageworks, Cambridge, MA).

**Projection Photolithography with the Microscope.** *Configuration of Optical Microscope.* The microscope used for all experiments was a Leica DMRX upright microscope with a reflected light path. The light source was a 100 W Hg gas discharge lamp. Typically, the power of the lamp was set to 80 W for exposures of the 1800 series resists and 100 W for the SU-8 resists. The objectives used were a  $40\times$  dry objective (Leitz, infinity-corrected, PLAN, NA = 0.60) and a  $100\times$  water immersion objective (Leitz, infinity-corrected, PLAN, NA = 1.2–0.45). For exposures using the immersion objective, a standard glass coverslip ( $\#1$ ,  $0.17\ \text{mm}$ ) was used to protect the photoresist from contact with the water. (Prolonged exposure to solvent vapors can adversely affect the quality of the image transferred to the resist layer, but we did not observe any solvent spots in the developed photoresist due to the presence of the water droplet.) The photomask was inserted into the field stop at the front of the diaphragm module (HC RF). No special modifications were made to the internal optical path of the microscope. An infrared hot mirror (Edmund Industrial Optics, Barrington, NJ) was placed in front of the light source to minimize heating (melting) of the transparency mask during exposures.

Adjusting the aperture diaphragm controlled the intensity of the illumination. Typically, the lowest setting (0) was used for the 1800 series resists and a higher setting (4) for the SU-8 resists. The projected pattern was focused onto the photoresist sample on the microscope stage. Switching in and out a pair of neutral density filters to lower the illumination intensity controlled the exposure time. (A red glass filter can also be used to minimize exposure during aligning and focusing.)

*Exposing Positive Photoresist by MPP.* Silicon  $(100)$  substrates (Silicon Sense, NH) were prepared by sonication in acetone and then in methanol and dried in an oven for 20 min at  $180\ ^\circ\text{C}$ . The substrates were primed with HMDS for 10 s and spun-dry. The Microposit 1800 series photoresists were spun to the desired thickness. For patterning masters for microcontact printing, we used a  $1.3\ \mu\text{m}$  thick layer of 1813 (4000 rpm for 40 s). The photoresist-coated substrates were baked at  $105\ ^\circ\text{C}$  for 4 min. Exposure times and illumination intensities under the microscope varied with reduction power and aperture size on the mask. Typical exposure times for the positive resists are on the order of  $3\text{--}10\ \text{s}$  through the  $100\times$  objective and  $10\text{--}45\ \text{s}$  through the  $40\times$  objective. The samples were developed in 5:1 water: Microposit 351 concentrate for 45 s. To calibrate the exposure

time for a given sample and photomask, a dose array was exposed and developed to determine optimal conditions.

**Exposing of Negative Photoresist.** Silicon  $\langle 110 \rangle$  substrates (Silicon Sense, NH) were prepared as described for positive photoresist. The SU-8 resists (SU-8-2, SU-8-10, SU-8-25) were spun to the desired thickness and prebaked according to the datasheets provided by Microchem. Exposure times with the Hg lamp at 100 W varied from 3 to 4 min through the  $40\times$  objective. Samples were postbaked at  $105^\circ\text{C}$  for 5 min and developed in PGMEA with minimal agitation for 3–5 min. All steps, except for developing, were conducted in a darkroom.

**Fabrication of Microstructures by Soft Lithography. Replica Molding of Poly(dimethylsiloxane).** The photoresist masters generated by MPP were coated with (tridecafluoro-1,1,2,2-tetrahydrooctyl)-1-trichlorosilane (United Chemical Technologies, Bristol, PA) by vacuum deposition in a desiccator for 1 h. The coating prevents the PDMS from curing to the exposed silicon wafer and lowers the surface energy of the substrate to more easily remove the molded PDMS from the master. A prepolymer of PDMS (Sylgard 184, Dow Corning, Midland, MI) was prepared by the mixing the prepolymer components in a ratio of 10:1 as recommended by the manufacturer. The prepolymer was cast onto the masters and cured at  $70^\circ\text{C}$  for at least 1 h. After the PDMS was cured, the replica patterned in bas-relief was gently removed from the master by hand.

**Microcontact Printing.** The PDMS stamp was inked using a cotton swab wetted with a solution of 1-hexadecanethiol or 1-octadecanethiol (5 mM in ethanol for a hydrophobic SAM) or 1-mercaptohexadecanoic acid (5 mM in ethanol for a hydrophilic SAM). The stamp was dried under a stream of nitrogen for at least 30 s. For feature sizes around  $1\ \mu\text{m}$ , drying times of 1–2 min produced the best results. After drying, the stamp was brought into contact with the gold substrate for 5–10 s. For the substrates where the patterned SAM was transferred into the gold, the unprotected gold was etched using an iron cyanide etch solution ( $0.1\ \text{M Na}_2\text{S}_2\text{O}_3/0.01\ \text{M K}_3\text{Fe}(\text{CN})_6/0.001\ \text{M K}_4\text{Fe}(\text{CN})_6/1\ \text{M KOH}$ ).<sup>26</sup> Two-component patterned SAM surfaces for selective wetting were generated by dipping the printed substrates into a solution of a complementary thiol (1-hexadecanethiol or 1-mercaptohexadecanoic acid, 5 mM in ethanol) for 30–60 s following  $\mu\text{CP}$ .<sup>13,14</sup> The substrates were rinsed with ethanol and blown dry.

**Microtransfer Molding.** A photoresist master produced by MPP was used to cast a PDMS mold. The mold was oxidized for 20 s at 2 Torr in an oxygen plasma and coated with (tridecafluoro-1,1,2,2-tetrahydrooctyl)-1-trichlorosilane by vacuum deposition in a desiccator for 1 h. A UV-curable prepolymer (NOA-73,

Norland Products, Cranbury, NJ) was spread onto the stamp. The liquid prepolymer was filled into the relief features of the stamp using the edge of a small piece of PDMS as a scraper/wiper to remove the excess prepolymer. The filled mold was placed in contact with a silicon wafer or glass slide and lightly clamped in place. The polymer was cured under a UV lamp for 30 min at a distance of  $\sim 2\ \text{cm}$ . The PDMS mold was gently removed. Wetting the mold with ethanol before removing the mold helps to preserve micron-scale structures.

**Electrical Microcontact Printing.** A PDMS stamp was cast on a master patterned by MPP. The features on the master were  $1.3\ \mu\text{m}$  high, in 1813 photoresist. An adhesion layer of 7 nm of chromium, followed by a layer of 80 nm of gold, was evaporated onto the stamp in a thermal evaporator (Cryo Auto 306, Edward High Vacuum Int.). The 1–2 mm thick PDMS stamp was supported on a copper block and mounted a distance of  $>25\ \text{cm}$  from the thermal source to minimize heating and thermal expansion of the PDMS during evaporation; the metal film can buckle when the PDMS cools to room temperature and disrupt the continuity of the metal film.<sup>34</sup> A 70 nm thick layer of poly(methyl methacrylate) (2% PMMA in chlorobenzene, 950K, MicroChem, Newton, MA) was cast by spin-coating at 6000 rpm onto a p-type silicon wafer. The substrate was baked at  $90^\circ\text{C}$  for 1 h in a vacuum. A  $1\ \text{cm}^2$  square of the PMMA-coated wafer was placed into contact with the gold-coated stamp. A 15 V bias was applied between the silicon wafer and the gold electrode for 5 s to transfer charge into the polymer layer. The stamp was removed gently by hand. The surface potential was imaged using a modified atomic force microscope (Nanoscope IIIa MultiMode with Extender electronics module, Digital Instruments, Santa Barbara, CA).<sup>33</sup>

**Acknowledgment.** This research was supported by DARPA and used the MRSEC Shared Facilities supported by the NSF under Award DMR-9400396. The authors gratefully thank Emanuele Ostuni, Ming-Hsien Wu, Steve Metallo, and Eric Sanchez for helpful discussions and Michael Tinkham for the use of the AFM for the Kelvin probe measurements. J.C.L. thanks the DoD for a graduate fellowship. D.B.W. thanks the NSF for a graduate fellowship.

LA010655T

(34) Bowden, N.; Brittain, S.; Evans, A. G.; Hutchinson, J. W.; Whitesides, G. M. *Nature* **1998**, *393*, 146–149.